Inorg. Chem. **2008**, *47*, 2196−2204

New Members of a Class of Dinitrosyliron Complexes (DNICs): Interconversion and Spectroscopic Discrimination of the Anionic $\{Fe(NO)_2\}^9$ $[(NO)_2Fe(C_3H_3N_2)_2]^-$ and $[(NO)_2Fe(C_3H_3N_2)(SR)]^-$ ($C_3H_3N_2$ = Deprotonated Imidazole; R = ^{t}Bu, Et, Ph)

Hsiao-Wen Huang,[†] Chih-Chin Tsou,[†] Ting-Shen Kuo,[‡] and Wen-Feng Liaw*[,†]

Department of Chemistry, National Tsing Hua University, Hsinchu 30013, Taiwan, and Instrumentation Center, National Taiwan Normal University, Taipei, Taiwan

Received October 10, 2007

The anionic $\{Fe(NO)_2\}^9$ DNIC $[(NO)_2Fe(C_3H_3N_2)_2]^-$ (**2**) ($C_3H_3N_2$ = deprotonated imidazole) containing the deprotonated imidazole-coordinated ligands and DNICs $[(NO)_2Fe(C_3H_3N_2)(SR)]^-$ (R = ^{t}Bu (**3**), Et (**4**), Ph (**5**)) containing the mixed deprotonated imidazole−thiolate coordinated ligands, respectively, were synthesized by thiol protonation or thiolate(s) ligand-exchange reaction. The anionic $\{Fe(NO)_2\}^9$ DNICs **2**−**5** were characterized by IR, UV–vis, EPR, and single-crystal X-ray diffraction. The facile transformation among the anionic $\{Fe(NO)_2\}^9$ DNICs **2**−**5** and $[(NO)_2Fe(S^tBu)_2]^-$/$[(NO)_2Fe(SEt)_2]^-$/$[(NO)_2Fe(SPh)_2]^-$ was demonstrated in this systematic study. Of importance, the distinct electron-donating ability of thiolates serve to regulate the stability of the anionic $\{Fe(NO)_2\}^9$ DNICs and the ligand-substitution reactions of DNICs. At 298 K, DNIC **2** exhibits the nine-line EPR signal with g = 2.027 ($a_{N(NO)}$ = 2.20 and $a_{N(Im\text{-}H)}$ = 3.15 G; Im-H = deprotonated imidazole) and DNIC **3** displays the nine-line signals with g = 2.027 ($a_{N(NO)}$ = 2.35 and $a_{N(Im\text{-}H)}$ = 4.10 G). Interestingly, the EPR spectrum of complex **4** exhibits a well-resolved 11-line pattern with g = 2.027 ($a_{N(NO)}$ = 2.50, $a_{N(Im\text{-}H)}$ = 4.10 G, and a_H = 1.55 G) at 298 K. The EPR spectra (the pattern of hyperfine splitting) in combination with IR ν_{NO} spectra ($\Delta\nu_{NO}$ = the separation of NO stretching frequencies, $\Delta\nu_{NO}$ = ∼62 cm^{-1} for **2** vs ∼50 cm^{-1} for **3**−**5** vs ∼43 cm^{-1} for $[(NO)_2Fe(S^tBu)_2]^-$/$[(NO)_2Fe(SEt)_2]^-$/$[(NO)_2Fe(SPh)_2]^-$) may serve as an efficient tool for the discrimination of the existence of the anionic $\{Fe(NO)_2\}^9$ DNICs containing the different ligations [N,N]/[N,S]/[S,S].

Introduction

In vivo, nitric oxide can be stabilized and stored in the form of dinitrosyliron complexes with proteins (protein-bound DNICs) and is probably released from cells in the form of low-molecular-weight dinitrosyliron complexes (low-molecular-weight DNICs (LMW-DNICs)).[1] Dinitrosyl iron complexes (DNICs) and *S*-nitrosothiols (RSNO) are known to be two possible forms for storage and transport of NO in biological systems.[2,3] Characterization of both protein-bound and low-molecular- weight DNICs in vitro has been made possible via their distinctive EPR signals at g = 2.03.[1−3]

* To whom correspondence should be addressed. E-mail: wfliaw@mx.nthu.edu.tw.

[†] National Tsing Hua University.

[‡] National Taiwan Normal University.

(1) (a) Lancaster, J. R., Jr.; Hibbs, J. B., Jr *Proc. Natl. Acad. Sci. U.S.A.* **1990**, *87*, 1223–1227. (b) Foster, M. W.; Cowan, J. A. *J. Am. Chem. Soc.* **1999**, *121*, 4093–4100. (c) Cooper, C. E. *Biochim. Biophys. Acta* **1999**, *1411*, 290–309. (d) Frederik, A. C.; Wiegant, I. Y.; Malyshev, I. Y.; Kleschyov, A. L.; van Faassen, E.; Vanin, A. F. *FEBS Lett.* **1999**, *455*, 179–182. (e) Butler, A. R.; Megson, I. L. *Chem. Rev.* **2002**, *102*, 1155–1166. (f) Hayton, T. W.; Legzdins, P.; Sharp, W. B. *Chem. Rev.* **2002**, *102*, 935–991. (g) Ueno, T.; Susuki, Y.; Fujii, S.; Vanin, A. F.; Yoshimura, T. *Biochem. Pharmacol.* **2002**, *63*, 485–493. (h) McCleverty, J. A. *Chem. Rev.* **2004**, *104*, 403–418.

(2) (a) Mülsch, A.; Mordvintcev, P. I.; Vanin, A. F.; Busse, R. *FEBS Lett.* **1991**, *294*, 252–256. (b) Badorff, C.; Fichtlscherer, B.; Muelsch, A.; Zeiher, A. M.; Dimmeler, S. *Nitric Oxide* **2002**, *6*, 305–312.

(3) (a) Stamler, J. S.; Singel, D. J.; Loscalzo, J. *Science* **1992**, *258*, 1898–1902. (b) Stamler, J. S. *Cell* **1994**, *78*, 931–936. (c) Frederik, A. C.; Wiegant, I. Y.; Malyshev, I. Y.; Kleschyov, A. L.; van Faassen, E.; Vanin, A. F. *FEBS Lett.* **1999**, *455*, 179–182. (d) Ford, P. C.; Lorkovic, I. M. *Chem. Rev.* **2002**, *102*, 993–1017. (e) Butler, A. R.; Megson, I. L. *Chem. Rev.* **2002**, *102*, 1155–1166. (f) Ueno, T.; Susuki, Y.; Fujii, S.; Vanin, A. F.; Yoshimura, T. *Biochem. Pharmacol.* **2002**, *63*, 485–493. (g) Lee, J.; Chen, L.; West, A. H.; Richter-Addo, G. B. *Chem. Rev.* **2002**, *102*, 1019–1065. (h) Hayton, T. W.; Legzdins, P.; Sharp, W. B. *Chem. Rev.* **2002**, *102*, 935–991. (i) Wang, P. G.; Xian, M.; Tang, X.; Wu, X.; Wen, Z.; Cai, T.; Janczuk, A. J. *Chem. Rev.* **2002**, *102*, 1091–1134. (j) McCleverty, J. A. *Chem. Rev.* **2004**, *104*, 403–418.

10.1021/ic702000y CCC: $40.75
Published on Web 02/14/2008

Table 1. Selected Spectroscopic Data for the Anionic/Neutral $\{Fe(NO)_2\}^9$ DNICs

complex	IR ν_{NO} (cm^{-1})	EPR (298 K)	EPR (4.2 K[c]/77 K[d])	ref
		Anionic $\{Fe(NO)_2\}^9$ DNICs		
$[(NO)_2FeS_5]^-$	1695, 1739[a]	2.03 (isotropic)	2.0485, 2.0270, 2.0148[c]	6d
$[(NO)_2Fe(2\text{-}S\text{-}(C_4H_3S)_2]^-$	1698, 1743[a]	2.027 ($A_N = 2.38$ G)		12
$[(NO)_2Fe(SC_6H_4\text{-}o\text{-}NHCOCH_3)_2]^-$	1705, 1752[a]	2,038 ($A_N = 2.27$ G)		12
$[(NO)_2Fe(S(CH_2)_3S)]^-$	1671, 1712[a]	2.031 (isotropic)	2.048, 2.033, 2.015[d]	6a
$[(NO)_2Fe(SC_6H_4\text{-}o\text{-}NHCOPh)_2]^-$	1705, 1752	2.0288 ($A_N = 2.344$G)		6b
$[(NO)_2Fe(SEt)_2]^-$	1674, 1715[a]	2.028 (isotropic)	2.042, 2.027, 2.014[d]	16a
$[(NO)_2Fe(SC_6H_4\text{-}o\text{-}NCOPh)]^-$	1690, 1737[b]	2.034 (isotropic)	2.052, 2.033, 2.011[d]	15
$[(SC_6H_4\text{-}o\text{-}COO)Fe(NO)_2]^-$	1688, 1742[a]	2.034 (isotropic)	2.054, 2.036, 2.012[d]	15
$[(NO)_2Fe(S^tBu)_2]^-$	1672, 1715[a]	2.029 ($A_N = 2.7$ G)	2.039, 2.027, 2.013[d]	16b
		Neutral/Dimeric $\{Fe(NO)_2\}^9$ DNICs		
$[(NO)_2Fe(SC_6H_4\text{-}o\text{-}NHCOPh)(Im)]$	1722, 1786	2.031 ($A_{N(NO)} = 2.4$ G, $A_{N(Im)} = 4.1$ G)		6b
$[Fe(\mu\text{-}SC_7H_4SN)(NO)_2]_2$	1736, 1789	2.033 (isotropic)	2.042, 2.033, 2.013[d]	15

[a] Cation = $[PPN]^+$. [b] Cation = $[Na^+$-18-crown-6-ether]. [c] 4.2 K. [d] 77 K.

Although cysteine and glutathione have been proposed to be the major thiol components of cellular DNICs in vivo, four different kinds of potential coordinated ligands (thiolate, imidazole, deprotonated imidazole, and phenoxide) in DNICs, based on EPR spectra, were proposed in enzymology.[4] In the inactivation of aconitase, upon addition of NO to the 3Fe form of *m*-aconitase, new transient signals, tentatively assigned as the formation of a DNIC containing two histidyl ligands or a DNIC containing the mixed ligands from both histidine and cysteine, appear during the early phases of the reaction.[4a] Compared to the EPR signals ($g_x = 2.055$, $g_y = 2.035$, $g_z = 2.01$ for $[BSA\text{-}(His)_2]Fe(NO)_2$ and $g_x = 2.05$, $g_y = 2.04$, $g_z = 2.01$ for $[BSA\text{-}(His)(Cys)]Fe(NO)_2$) observed in the reaction of bovine serum albumin and L-cysteine DNIC,[4b] the EPR signals of $g_x = 2.055$, $g_y = 2.033$, and $g_z = 2.015$ observed in the studies of reaction of mammalian ferritin and NO were also attributed to the formation of a histidyl−iron nitrosyl or a histidyl−thiol−iron nitrosyl complex.[4c] More recently, FeFur (ferric uptake regulation protein) treated by NO was proposed to lead to an Fur-bound $\{Fe(NO)_2\}^9$ iron nitrosyl complex without bound thiolates because the site-directed mutagenesis reveals that neither of the two cysteines is required for the formation of the $g = 2.03$ signal.[5]

On the basis of oxidation levels of the $\{Fe(NO)_2\}$ core of DNICs, DNICs can be classified into the EPR-active anionic $\{Fe(NO)_2\}^9$, neutral $\{Fe(NO)_2\}^9$, and cationic $\{Fe(NO)_2\}^9$ DNICs and into the EPR-silent, neutral $\{Fe(NO)_2\}^{10}$ DNICs in inorganic chemistry.[6–9] Here, the electronic state of the $\{Fe(NO)_2\}$ unit of DNICs is generally designated as $\{Fe(NO)_2\}^n$. This formalism $\{M(NO)_2\}^n$ (M = transition metal), in which *n* is the total number of electrons associated with the metal d and π^*(NO) orbitals, follows the Enemark−Feltham notation.[10]

Recently, we have established that the IR ν_{NO} in combination with EPR spectra (pattern) may be employed to discriminate the $\{Fe(NO)_2\}^9$ DNICs with a variety of coordinated ligands (thiolate, imidazole, amide, and carboxylate) (Table 1). In addition, we also showed that neutral $\{Fe(NO)_2\}^{10}$ [(sparteine)$Fe(NO)_2$] easily converts to the anionic $\{Fe(NO)_2\}^9$ $[(S(CH_2)_3S)Fe(NO)_2]^-$ via the cationic $\{Fe(NO)_2\}^9$ $[(sparteine)Fe(NO)_2]^+$.[6a] Conversion of Roussin's red esters (RRE) $[Fe(\mu\text{-}SC_6H_4\text{-}o\text{-}NHCOPh)(NO)_2]_2$ into the neutral $\{Fe(NO)_2\}^9$ $[(SC_6H_4\text{-}o\text{-}NHCOPh)(Im)Fe(NO)_2]$ (Im = imidazole) was demonstrated by reaction of $[Fe(\mu\text{-}SC_6H_4\text{-}o\text{-}NHCOPh)(NO)_2]_2$ with imidazole.[6b] Transformations of RREs $[Fe(\mu\text{-}SC_6H_4\text{-}o\text{-}NHCOPh)(NO)_2]_2$ and $[Fe(\mu\text{-}SC_6H_4\text{-}o\text{-}COOH)(NO)_2]_2$ into (i) the neutral $\{Fe(NO)_2\}^{10}$, $[(PPh_3)_2Fe(NO)_2]$ via reductive elimination of the bridged thiolates, and (ii) the anionic $\{Fe(NO)_2\}^9$ $[(SC_6H_4\text{-}o\text{-}NCOPh)Fe(NO)_2]^-$ and $[(SC_6H_4\text{-}o\text{-}COO)Fe(NO)_2]^-$ incorporating anionic sulfur−amide and sulfur−carboxylate chelates, respectively, controlled by the nucleophile L (L = PPh_3, $[OPh]^-$) were elucidated through reaction of RREs with the nucleophile L.[6c] Although a number of dinitrosyliron complexes have been proposed to contain [N,N]-coordinated ligands (Table 2), no mononuclear DNICs coordinated to deprotonated imidazoles or the mixed deprotonated imidazole−thiolate ligands have been well characterized.[11] The objective of this study was to delineate the synthesis, reactivity, and interconversion of the EPR-active, anionic $\{Fe(NO)_2\}^9$ $[(NO)_2Fe(C_3H_3N_2)_2]^-$ ($C_3H_3N_2$ = deprotonated imidazole) (**2**) and $[(NO)_2Fe(C_3H_3N_2)(SR)]^-$ (R = ^{t}Bu (**3**), Et (**4**), Ph (**5**)) containing the deprotonated imidazole or the

(4) (a) Kennedy, M. C.; Antholine, W. E.; Beinert, H. J. *Biol. Chem.* **1997**, *272*, 20340–20347. (b) Boese, M.; Mordvintcev, P. I.; Vanin, A. F.; Busse, R.; Mulsch, A. *J. Biol. Chem.* **1995**, *207*, 29244–29249. (c) Lee, M.; Arosio, P.; Cozzi, A.; Chasteen, N. D. *Biochemistry* **1994**, *33*, 3679–3687.

(5) D'Autréaux, B.; Horner, O.; Oddou, J.-L.; Jeandey, C.; Gambarelli, S.; Berthomieu, C.; Latour, J.-M.; Michaud-Soret, I. *J. Am. Chem. Soc.* **2004**, *126*, 6005–6016.

(6) (a) Hung, M.-C.; Tsai, M.-C.; Lee, G.-H.; Liaw, W.-F. *Inorg. Chem.* **2006**, *45*, 6041–6047. (b) Tsai, M.-L.; Liaw, W.-F. *Inorg. Chem.* **2006**, *45*, 6583–6585. (c) Tsai, M.-L.; Hsieh, C.-H.; Liaw, W.-F. *Inorg. Chem.* **2007**, *46*, 5110–5117. (d) Tsai, M.-L.; Chen, C.-C.; Hsu, I.-J.; Ke, S.-C.; Hsieh, C.-C.; Chiang, K.-A.; Lee, G.-H.; Wang, Y.; Chen, J.-M.; Lee, J.-F.; Liaw, W.-F. *Inorg. Chem.* **2004**, *43*, 5159–5167.

(7) (a) Baltusis, L. M.; Karlin, K. D.; Rabinowitz, H. N.; Dewan, J. C.; Lippard, S. J. *Inorg. Chem.* **1980**, *19*, 2627–2632. (b) Chiang, C.-Y.; Miller, M. L.; Reibenspies, J. H.; Darensbourg, M. Y. *J. Am. Chem. Soc.* **2004**, *126*, 10867–10874.

(8) Albano, V. G.; Araneo, A.; Bellon, P. L.; Ciani, G.; Manassero, M. *J. Organomet. Chem.* **1974**, *67*, 413–422.

(9) Reginato, N.; McCrory, C. T. C.; Pervitsky, D.; Li, L. *J. Am. Chem. Soc.* **1999**, *121*, 10217–10218.

(10) Enemark, J. H.; Feltham, R. D. *Coord. Chem. Rev.* **1974**, *13*, 339–406.

(11) (a) Martini, G.; Tiezzi, E. *Z. Naturtorsch.* **1973**, *28b*, 300–305. (b) Tiezzi, E.; Niccolai, N.; Basosi, R. *J. Chim. Phys.* **1977**, *74*, 559–562. (c) Jezowska-Trezebiatowska, B.; Jezierski, A. J. *Mol. Struct.* **1973**, *19*, 635–640.

Table 2. Proposed DNICs (*Italic*) and Single-Crystal X-ray Structure Characterized DNICs (**Bold**) with N-Coordinated Ligands (Im-H = Deprotonated Imidazole)

compd	*g* value	no. lines in hyperfine splitting	a_N (G)	ref
$(NO)_2Fe(imidazole)_2$	2.026	9	2.7	11a
	2.027[b]		2.0 (NO)	11b
			2.7 (Im)	
$[(NO)_2Fe(C_3H_3N_2)_2]^-$	2.027	9	2.20 (NO)	this work
			3.15 (Im-H)	
$(NO)_2Fe(adenine)$	2.028[b]	9		11b
$(NO)_2Fe(DNA)$	2.028[b]	9		11b
$(NO)_2Fe(RNA^c)$	2.028[b]	9		11a
iron nitrosyl N-ethylimidazole complex	2.027	9	2.5	11c
$(NO)_2Fe(1\text{-}MeIm)_2^+$	2.0151	9	3.6 (N_1)	9
			3.9 (N_2)	
$[Fe(NO)_2(imidazole)]_4$	2.031[d]	9	3.54 (N_1)	13
			4.5 (N_2)	
$(NO)_2Fe(SC_6H_4\text{-}NHCOPh)(Im)$				
	2.031	9	2.4 (NO)	6b
			4.1 (Im)	
$[(NO)_2Fe(C_3H_3N_2)(S^tBu)]^-$	2.027	9	2.35 (NO)	this work
			4.10 (Im-H)	
$[(NO)_2Fe(C_3H_3N_2)(SEt)]^-$	2.027	11	2.50 (NO)	this work
			4.10 (Im-H)	
			1.55 (SCH_2)	
$[(NO)_2Fe(C_3H_3N_2)(SPh)]^-$	2.027	7		this work
$(^{15}NO)_2Fe(histamine)$	2.033	5		11b
$(NO)_2Fe(carbohydrazide)$	2.0207	9[a]	2.7 (NO)	11a
			7 (NH_2)	
	2.045	13[b]	2.1 (NO)	11a
			4.3 (NH)	

[a] At pH < 7. [b] At pH > 7. [c] From yeast. [d] 170 K.

mixed deprotonated imidazole−thiolate ligands. We demonstrate that thiolates regulate the stability and reactivity of the anionic $\{Fe(NO)_2\}^9$ DNICs. In particular, the detailed spectroscopic analysis (EPR and IR ν_{NO} spectra) may provide a superior level of insight on discrimination of the anionic $\{Fe(NO)_2\}^9$ DNICs **2–5** and $[(NO)_2Fe(SR)_2]^-$ complexes.

Results and Discussion

Synthesis of [Na-18-crown-6-ether][$(NO)_2Fe(C_3H_3N_2)_2$] (2). As reported in the previous study, the coordinated ligands $[-SC_7H_4SN]^-$ (2-benzothiozoyl thiolates) of the anionic $\{Fe(NO)_2\}^9$ [Na-18-crown-6-ether][$(NO)_2Fe(SC_7H_4SN)_2$] (**1**) may be replaced by the stronger electron-donating thiolate ligands $[SPh]^-$ to yield the stable $[(NO)_2Fe(SPh)_2]^-$.[12] Complex **1** and 2 equiv of sodium imidazole [Na][$C_3H_3N_2$] ($C_3H_3N_2$ = deprotonated imidazole = Im-H) were stirred in THF at ambient temperature overnight. The crimson solution turned dark-brown. The shift in IR ν_{NO} from 1767 and 1717 s cm^{-1} to 1774 and 1712 s cm^{-1} is consistent with the formation of the $\{Fe(NO)_2\}^9$ [Na-18-crown-6-ether][$(NO)_2Fe(C_3H_3N_2)_2$] (**2**), which was characterized by UV–vis, EPR, and single-crystal X-ray diffraction (Scheme 1a). In comparison with the nine-line EPR spectrum of the neutral $\{Fe(NO)_2\}^9$ DNIC [$(SC_6H_4$-*o*-NHCOPh)(Im)$Fe(NO)_2$] (Im = imidazole) with $g = 2.031$ and the hyperfine coupling constants $a_{N(NO)} = 2.4$ and $a_{N(Im)} = 4.1$ G,[6b] complex **2** exhibits the nine-line EPR signal with $g = 2.027$ at 298 K. The value $g = 2.027$ and the hyperfine

Scheme 1

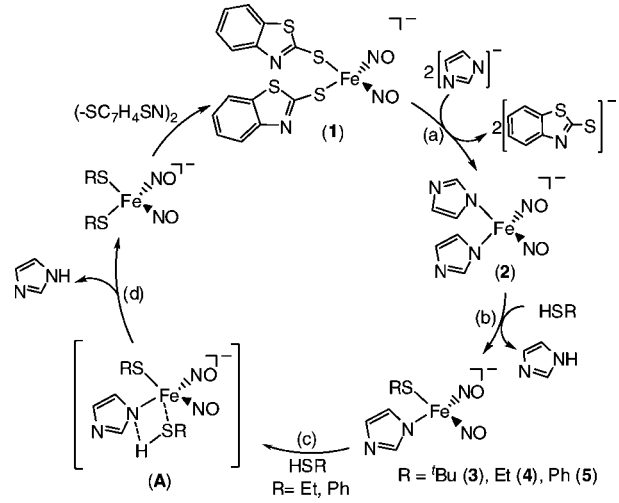

coupling constants $a_{N(NO)} = 2.20$ and $a_{N(Im\text{-}H)} = 3.15$ G (Figure 1) are characteristic of anionic $\{Fe(NO)_2\}^9$ DNICs. At 77 K, complex **2** displays the rhombic EPR spectrum with $g_1 = 2.040$, $g_2 = 2.022$, and $g_3 = 2.013$ (Figure 1b). Compared to the cyclic tetranuclear dinitrosyliron complex $[Fe(NO)_2(imidazolate)]_4$ reported by Li and co-workers,[13] complex **2** is the first example of the mononuclear anionic $\{Fe(NO)_2\}^9$ DNICs containing the deprotonated imidazoles coordinated to the $\{Fe(NO)_2\}^9$ motif and characterized by single-crystal X-ray diffraction.

(12) Tsai, F.-T.; Chiou, S.-J.; Tsai, M.-C.; Tsai, M.-L.; Huang, H.-W.; Chiang, M.-H.; Liaw, W.-F. *Inorg. Chem.* **2005**, *44*, 5872–5881.

(13) Wang, X.; Sundberg, E. B.; Li, L.; Kantardjieff, K. A.; Herron, S. R.; Lim, M.; Ford, P. C. *Chem. Commun.* **2005**, *477*, 479.

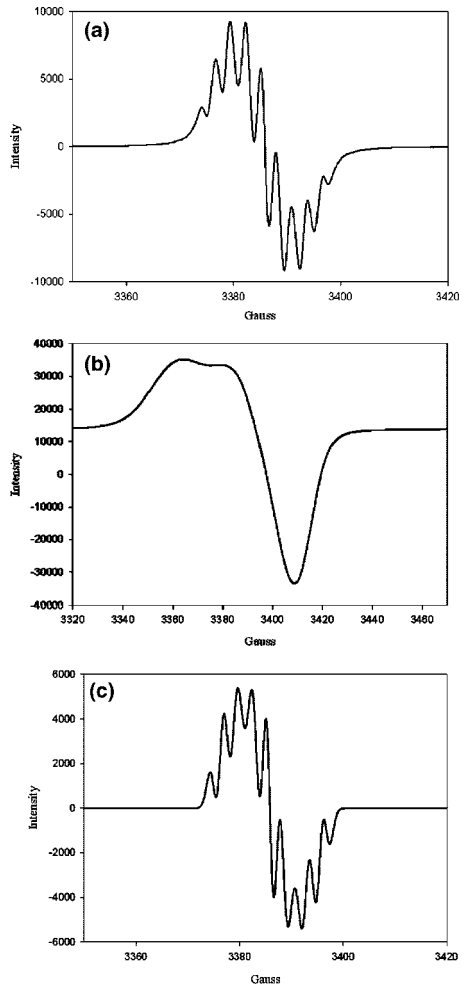

Figure 1. EPR spectra of complex **2** (a) at 298 K ($g = 2.027$), (b) at 77 K ($g_1 = 2.040$, $g_2 = 2.022$, and $g_3 = 2.013$), and (c) the simulated EPR spectrum of complex **2** with hyperfine coupling constants of $a_{N(NO)} = 2.20$ G and $a_{N(Im-H)} = 3.15$ G.

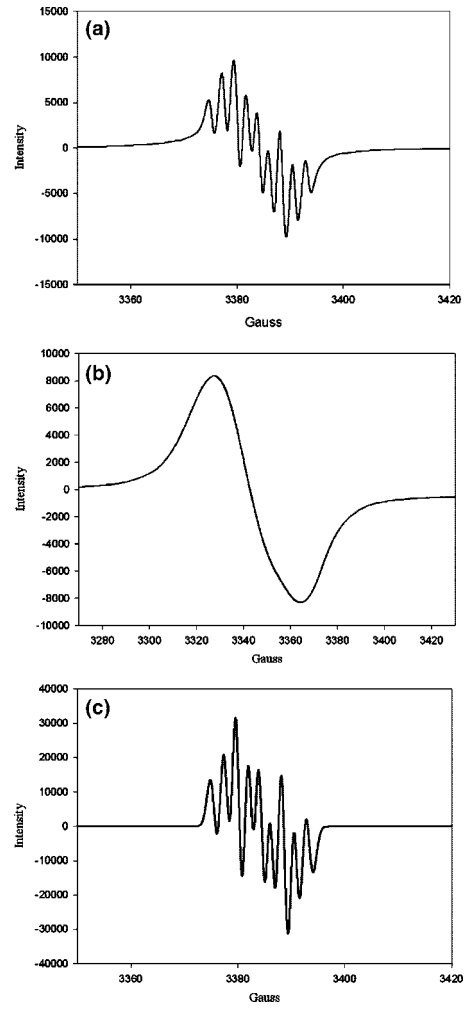

Figure 2. EPR spectra of complex **3** (a) at 298 K ($g = 2.027$), (b) at 77 K ($g_1 = 2.037$, $g_2 = 2.027$, and $g_3 = 2.014$), and (c) the simulated EPR spectrum of complex **3** with hyperfine coupling constants of $a_{N(NO)} = 2.35$ G and $a_{N(Im-H)} = 4.10$ G.

Reaction of [Na-18-crown-6-ether][$(NO)_2Fe(C_3H_3N_2)_2$] (2) and Thiols. In order to elucidate the stability and reactivity of complex **2** and synthesize dinitrosyliron complexes with the mixed deprotonated imidazole−thiolate ligands, reactions of complex **2** and thiols were investigated. The *tert*-butylthiol diluted in THF was slowly injected into the THF solution of complex **2** at room temperature. The IR ν_{NO} stretching frequencies (ν_{NO}, 1741 s, 1690 s cm^{-1} (THF)) imply the formation of [Na-18-crown-6-ether][$(NO)_2Fe(C_3H_3N_2)(S^tBu)$] (**3**) coordinated by the deprotonated imidazole and thiolate ligands (Scheme 1b). The lower energy ν_{NO} bands of complex **3** shifted by $\sim$30 cm^{-1} from that of complex **2** (ν_{NO}, 1774 s, 1712 s cm^{-1} (THF)), which is consistent with the weaker electron-donating character of the deprotonated imidazole $[C_3H_3N_2]^-$ ligand, compared to $[S^tBu]^-$. Complex **3** was characterized by UV–vis, IR, EPR, SQUID, and single-crystal X-ray diffraction. The conversion of complex **2** to complex **3** is presumed to occur via protonation (*tert*-butylthiol) of one deprotonated imidazole-coordinated ligand of complex **2** (14.52 (pK_{a2} of imidazole) vs 11.05 (pK_a of *tert*-butylthiol))[14] and the subsequent coordination of $[S^tBu]^-$. The EPR spectrum of complex **3** exhibits a nine-line spectrum with $g = 2.027$ and the hyperfine coupling constants $a_{N(NO)} = 2.35$ G and $a_{N(Im-H)} = 4.10$ G at 298 K (Figure 2) and a rhombic signal with $g_1 = 2.037$, $g_2 = 2.027$, and $g_3 = 2.014$ at 77 K (Figure 2b). Magnetic susceptibility data of a powder sample of complex **3** were collected in the temperature range of 2.00–300 K in 5 kG (0.5 T). The net molar magnetic susceptibility (χ_M) increased from 1.79×10^{-3} cm^3 mol^{-1} at 300 K to 0.180 cm^3 mol^{-1} at 2 K. The temperature-dependent effective magnetic moment (μ_{eff}) decreases from 2.073 μ_B at 300 K to 1.697 μ_B at 2 K (Figure 3).[12,15]

In a similar fashion, upon addition of 1 equiv of the THF-diluted ethylthiol to the THF solution of complex **2**, a pronounced color change from dark-brown to yellow-brown occurs at ambient temperature. The IR, UV–vis, EPR, and single-crystal X-ray diffraction studies confirmed the formation of the anionic $\{Fe(NO)_2\}^9$ $[(NO)_2Fe(C_3H_3N_2)(SEt)]^-$ (**4**) with the anionic $[SEt]^-$ and $[C_3H_3N_2]^-$ ligands bound to the

(14) (a) Walba, H.; Isensee, R. W. *J. Am. Chem. Soc.* **1955**, *77*, 5488–5492. (b) Bruice, T. C.; Schmir, G. L. J. *Am. Chem. Soc.* **1958**, *80*, 148–156.

(15) Tsai, M.-L.; Chen, C.-C.; Hsu, I.-J.; Ke, S.-C.; Hsieh, C.-H.; Chiang, K.-A.; Lee, G.-H.; Wang, Y.; Chen, J.-M.; Lee, J.-F.; Liaw, W.-F. *Inorg. Chem.* **2004**, *43*, 5159–5167.

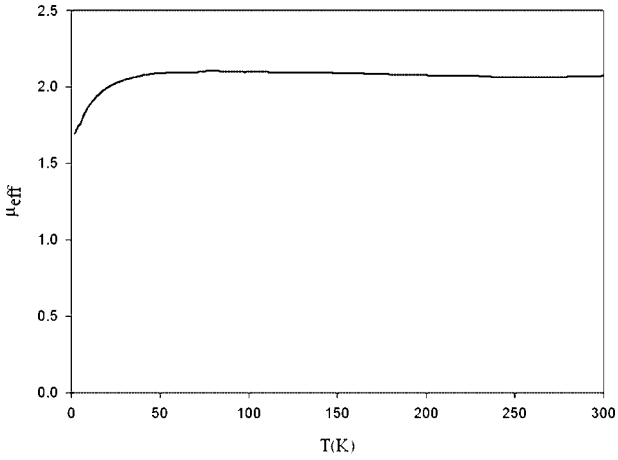

Figure 3. Plots of effective magnetic moment vs temperature for complex **3**.

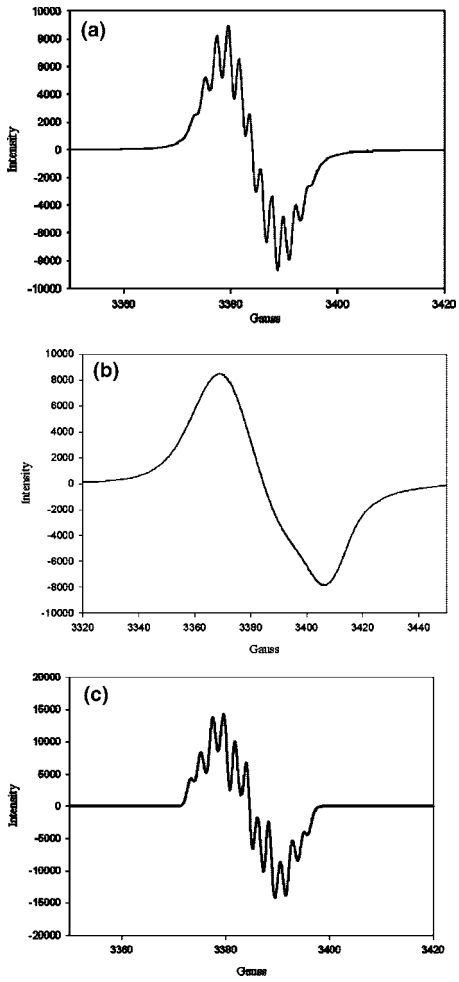

Figure 4. EPR spectra of complex **4** (a) at 298 K ($g = 2.027$), (b) at 77 K ($g_1 = 2.037$, $g_2 = 2.028$, and $g_3 = 2.014$), and (c) the simulated EPR spectrum of complex **4** with hyperfine coupling constants of $a_{N(NO)} = 2.50$ G, $a_{N(Im\text{-}H)} = 4.10$ G, and $a_{H(SCH2)} = 1.55$ G.

$\{Fe(NO)_2\}$ core (Scheme 1b). In comparison with the nine-line spectrum observed in complex **3**, complex **4** exhibits a well-resolved 11-line EPR signal with $g = 2.027$ and the hyperfine splitting constants ($a_{N(NO)} = 2.50$ G, $a_{N(Im\text{-}H)} = 4.10$ G, and $a_{H(SCH2\text{-})} = 1.55$ G) at 298 K (Figure 4). The EPR splitting lines of complex **4** can be rationalized by the unpaired electron coupling with 3′-N of the deprotonated imidazole-coordinated ligand, the nitrosyl groups, and H atoms of the coordinated $S-CH_2-Me$ group. At 77 K, the EPR spectrum of complex **4** shows a rhombic signal with $g_1 = 2.037$, $g_2 = 2.028$, $g_3 = 2.014$. In a similar fashion, reaction of complex **2** and HSPh produced [Na-18-crown-6-ether][$(NO)_2Fe(C_3H_3N_2)(SPh)$] (**5**) (ν_{NO}, 1708 s, 1760 s cm^{-1} (THF)) characterized by IR, UV–vis, and single-crystal X-ray diffraction.

Further protonation of complexes **4** and **5** by EtSH and PhSH, respectively, results in the formation of the well-known $\{Fe(NO)_2\}^9$ DNICs $[(NO)_2Fe(SEt)_2]^-$ and $[(NO)_2Fe(SPh)_2]^-$ in THF at ambient temperature (Scheme 1c).[12,16] Here, protonation of DNICs **4** and **5** is presumed to occur only at the more accessible, electron-rich N site leading to the formation of the proposed intermediate **A** (Scheme 1), placing the $\{Fe(NO)_2\}$ core in an optimum electronic condition, and subsequently leads to production of the well-known $\{Fe(NO)_2\}^9$ $[(NO)_2Fe(SR)_2]^-$ (R = Et, Ph). In contrast, DNIC **3** does not react with *tert*-butylthiol in a 1:1 molar ratio to yield the well-known $[(NO)_2Fe(S^tBu)_2]^-$.[15,17] The inertness of complex **3** toward *tert*-butylthiol is ascribed to the steric hindrance of the coordinated $[S^tBu]^-$ and the deprotonated imidazole ligands of complex **3**, which is resistant to further protonation to produce the intermediate **A** (Scheme 1c) and trigger the subsequent ligand displacement. The steric effect of the coordinated ligands in the coordination sphere from complex **3** to $[(NO)_2Fe(S^tBu)_2]^-$ overwhelms the electronic effect expected in the ligand-displacement reaction of DNICs, which may explain the observed inertness of complex **3** toward HS^tBu. Thus, the bulky $[S^tBu]^-$-coordinated ligand of complex **3** may promote the stability of the $\{Fe(NO)_2\}^9$ DNICs **3**, compared to the ethylthiolate- and phenylthiolate-coordinated DNICs **4** and **5**.

It is noted that the IR spectra among DNICs **2**−**5** and $[(NO)_2Fe(SPh)_2]^-/[(NO)_2Fe(SEt)_2]^-$ had the same pattern but differed in the position (1712 and 1774 cm^{-1} for **2** vs 1691 and 1742 cm^{-1} for **3** vs 1693 and 1743 cm^{-1} for **4** vs 1708 and 1760 cm^{-1} for **5** vs 1672 and 1715 cm^{-1} for $[(NO)_2Fe(S^tBu)_2]^-$ vs 1674 and 1714 cm^{-1} for $[(NO)_2Fe(SEt)_2]^-$ and vs 1695 and 1739 cm^{-1} for $[(NO)_2Fe(SPh)_2]^-$) and the separation of NO stretching frequencies $\Delta\nu_{NO}$ ($\Delta\nu_{NO}$, ~62 cm^{-1} for **2** vs ~50 cm^{-1} for **3**−**5** vs ~43 cm^{-1} for $[(NO)_2Fe(S^tBu)_2]^-/[(NO)_2Fe(SEt)_2]^-/[(NO)_2Fe(SPh)_2]^-$). The results obtained from this work suggest that the EPR spectrum (the pattern of hyperfine splitting) in combination with IR $\Delta\nu_{NO}$ spectrum (ν_{NO}, ~62 cm^{-1} for the anionic $\{Fe(NO)_2\}^9$ [N,N]-ligation mode of DNICs, ~50 cm^{-1} for the anionic $\{Fe(NO)_2\}^9$ [N,S]-ligation mode of DNICs, and ~43 cm^{-1} for the anionic $\{Fe(NO)_2\}^9$ [S,S]-ligation mode of DNICs) may serve as an efficient tool for the discrimination of the existence of the anionic $\{Fe(NO)_2\}^9$ DNICs containing the variety of [N,N]/[N,S]/[S,S] ligations.

(16) (a) Lu, T.-T.; Chiou, S.-J.; Chen, C.-Y.; Liaw, W.-F. *Inorg. Chem.* **2006**, *45*, 8799–8806. (b) Tsou, C.-C.; Lu, T.-T.; Liaw, W.-F. *J. Am. Chem. Soc.* **2007**, *129*, 12626–12627. (c) Strasdeit, H.; Krebs, B.; Henkel, G. *Z. Naturforsch.* **1986**, *41b*, 1357.

(17) Harrop, T. C.; Song, D.; Lippard, S. J. J. *Am. Chem. Soc.* **2006**, *128*, 3528–3529.

Scheme 2

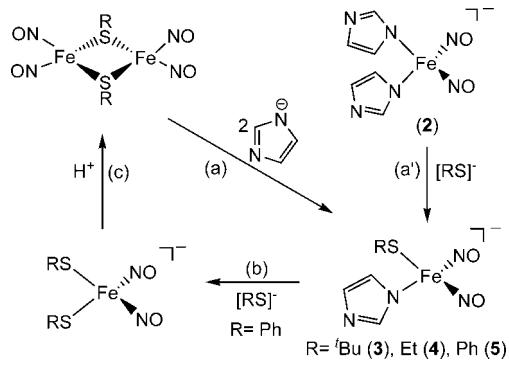

Alternative Synthetic Route to Complexes 3−5. The transformation of Roussin's red ester $[Fe(\mu\text{-}SC_6H_4\text{-}o\text{-}NHCOPh)(NO)_2]_2$ into the neutral $\{Fe(NO)_2\}^9$ $[(SC_6H_4\text{-}o\text{-}NHCOPh)(Im)Fe(NO)_2]$ (Im = imidazole) was demonstrated by the reaction of $[Fe(\mu\text{-}SC_6H_4\text{-}o\text{-}NHCOPh)(NO)_2]_2$ with 2 equiv of imidazole.[6b] In contrast to the deprotonation of the bridged thiolates yielding $[(SC_6H_4\text{-}o\text{-}NCOPh)Fe(NO)_2]^-$ and $[(SC_6H_4\text{-}o\text{-}COO)Fe(NO)_2]^-$ observed in the reaction of complexes $[Fe(\mu\text{-}SC_6H_4\text{-}o\text{-}NHCOPh)(NO)_2]_2$/$[Fe(\mu\text{-}SC_6H_4\text{-}o\text{-}COOH)(NO)_2]_2$ and 2 equiv of $[OPh]^-$, respectively,[6c] the addition of 2 equiv of [Na-18-crown-6-ether]$[C_3H_3N_2]$ to complexes $[Fe(\mu\text{-}SR)(NO)_2]_2$ (R = ᵗBu, Et, Ph) in THF at ambient temperature led to the formation of complexes **3**, **4**, and **5**, respectively, via the bridged-thiolate cleavage (Scheme 2a). Alternatively, the deprotonated imidazole-coordinated ligand of DNIC **2** could be replaced by the stronger electron-donating thiolates $[SR]^-$ (R = ᵗBu, Et, Ph) to yield the stable complexes **3**−**5**, respectively (Scheme 2a′). The ligand displacement of the coordinated deprotonated imidazole of complex **2** is presumably ascribed to the electron-deficient $\{Fe(NO)_2\}$ core induced by the less electron-donating deprotonated imidazole-coordinated ligands. The electronic deficiency surrounding the $\{Fe(NO)_2\}$ core of complex **2** may promote the coordination of thiolate to yield the presumed intermediate $[(NO)_2Fe(C_3H_3N_2)_2(SR)]^{2-}$, and the subsequent elimination of the deprotonated imidazole-coordinated ligand leads to the DNICs **3**−**5**, respectively.

In contrast to the inertness of DNICs **3** and **4** toward $[SR]^-$ (R = ᵗBu, Et), reaction of DNIC **5** and 1 equiv of $[SPh]^-$ in THF solution at room temperature rapidly yielded the known $\{Fe(NO)_2\}^9$ DNICs $[(NO)_2Fe(SPh)_2]^-$ identified by IR and UV–vis (Scheme 2b). This result also confirms that the electron-deficient $\{Fe(NO)_2\}$ core of DNIC **5** caused by the weaker electron-donating $[SPh]^-$-coordinated ligand, compared to $[S^tBu]^-$ and $[SEt]^-$, triggers the coordination of $[SPh]^-$ to the $\{Fe(NO)_2\}$ core of complex **5**, and the subsequent elimination of the coordinated deprotonated imidazole yields $[(NO)_2Fe(SPh)_2]^-$. Conclusively, the distinct electron-donating ability of thiolates may serve to regulate the stability of DNICs and the ligand-substitution reaction of DNICs.

Structures. Crystals of complex **2** were obtained from nitrogen purge of CH_2Cl_2 solution of complex **2** at ambient temperature, and the structure of the $[(NO)_2Fe(C_3H_3N_2)_2]^-$ (**2**) unit containing packing solvent CH_2Cl_2 in [Na-18-crown-6-ether]$^+$ salt is shown in Figure 5. The $[(NO)_2Fe(C_3H_3N_2)_2]^-$ anion was held together by $Na^+\cdots[C_3H_3N_2]^-$ (3′-N of the coordinated deprotonated imidazole of complex **2**) interactions featuring a polymeric DNIC linked by the repeat unit of a [Na-18-crown-6-ether]$[(NO)_2Fe(C_3H_3N_2)_2]$ (Supporting Information Figure S1). The shorter Fe(1)−N(3) and Fe(1)−N(5) bond distances of 1.974(3) and 1.978(3) Å, respectively, compared to the reported $Fe-N_{(Im)}$ bond length of 2.021(4) Å in $[(SC_6H_4\text{-}o\text{-}NHCOPh)(Im)Fe(NO)_2]$,[6b] was attributed to the π-donating ability of the deprotonated imidazole $[C_3H_3N_2]^-$ ligands which stabilize the anionic $\{Fe(NO)_2\}^9$ complex **2**. The Fe(1)−N(1) and Fe(1)−N(2) bond lengths of 1.683(3) and 1.688(3) Å, respectively, also fall in the range 1.661(4)–1.695(3) Å observed in the anionic $\{Fe(NO)_2\}^9$ DNICs. Also, the nearly identical N(1)−O(1) and N(2)−O(2) bond lengths of 1.175(4) and 1.168(4) Å, respectively, are within the range 1.160(6)–1.178(3) Å observed for the anionic $\{Fe(NO)_2\}^9$ DNICs.[6a]

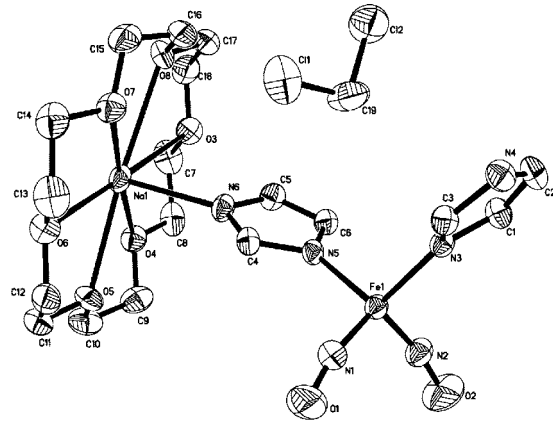

Figure 5. ORTEP drawing and labeling scheme of $[(NO)_2Fe(C_3H_3N_2)_2]^-$ (**2**) unit in [Na-18-crown-6-ether]$^+$ salt with thermal ellipsoids drawn at 50% probability. Selected bond distances (Å) and angles (deg) are as follows: Fe(1)−N(1) 1.683(3); Fe(1)−N(2) 1.688(4); Fe(1)−N(3) 1.974(3); Fe(1)−N(5) 1.978(3); O(1)−N(1) 1.175(4); O(2)−N(2) 1.168(4); N(1)−Fe(1)−N(2) 113.98(16); N(1)−Fe(1)−N(3) 108.43(13); N(2)−Fe(1)−N(3) 108.86(13); N(1)−Fe(1)−N(5) 108.48(13); N(2)−Fe(1)−N(5) 108.78(13); N(3)−Fe(1)−N(5) 108.16(12); O(1)−N(1)−Fe(1) 166.9(3); O(2)−N(2)−Fe(1) 166.2(3).

Figures 6−8 show the thermal ellipsoid plots of complexes **3**−**5**, and the selective bond distances and angles are given in the figures captions, respectively. The structure of $[C_4H_8O$-Na-18-crown-6-ether$][(NO)_2Fe(C_3H_3N_2)(S^tBu)]$ can be viewed in terms of the $[(NO)_2Fe(C_3H_3N_2)(S^tBu)]^-$ anion and $[C_4H_8O$-Na-18-crown-6-ether$]^+$ cation held together by $Na^+\cdots[C_3H_3N_2]^-$ (3′-N of the coordinated deprotonated imidazole of complex **3**) ionic interaction and the Na^+-O (THF) bond. It is noted that the reported average Fe−S bond lengths of 2.280(1), 2.274(2), and 2.2922(6) Å in $[(NO)_2Fe(S^tBu)_2]^-$, $[(NO)_2Fe(SEt)_2]^-$, and $[(NO)_2Fe(SPh)_2]^-$,[16] respectively, are significantly longer than the Fe(1)−S(1) distance of 2.237(2) Å in complex **3**, 2.2469(9) Å in complex **4**, and 2.265(2) Å in complex **5** (Table 3). The shortening in Fe−S bond lengths from 2.280(1)/2.274(2)/2.2922(6) Å for complexes $[(NO)_2Fe(S^tBu)_2]^-$/$[(NO)_2Fe(SEt)_2]^-$/$[(NO)_2Fe(SPh)_2]^-$ to

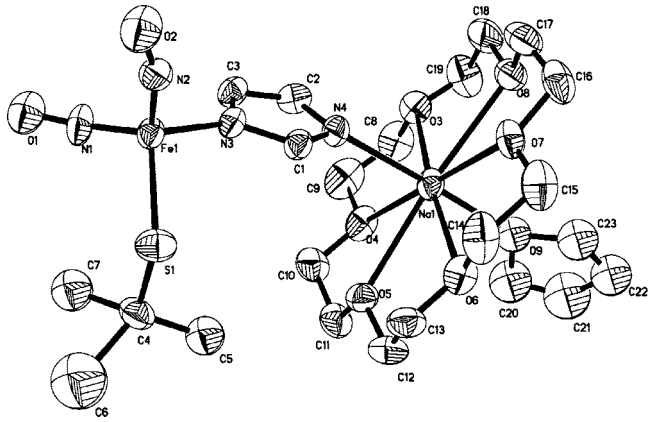

Figure 6. ORTEP drawing and labeling scheme of $[(NO)_2Fe(C_3H_3N_2)(S^tBu)]^-$ (**3**) unit in $[Na\text{-}18\text{-}crown\text{-}6\text{-}ether]^+$ salt with thermal ellipsoids drawn at 30% probability. Selected bond distances (Å) and angles (deg) are as follows: Fe(1)−N(1) 1.642(7); Fe(1)−N(2) 1.688(6); Fe(1)−N(3) 1.984(6); Fe(1)−S(1) 2.237(2); O(1)−N(1) 1.190(9); O(2)−N(2) 1.175(8); N(1)−Fe(1)−N(2) 115.7(3); N(1)−Fe(1)−N(3) 106.6(3); N(2)−Fe(1)−N(3) 111.6(3); N(1)−Fe(1)−S(1) 111.2(3); N(2)−Fe(1)−S(1) 102.7(2); N(3)−Fe(1)−S(1) 108.84(19); O(1)−N(1)−Fe(1) 169.7(7); O(2)−N(2)−Fe(1) 164.5(6).

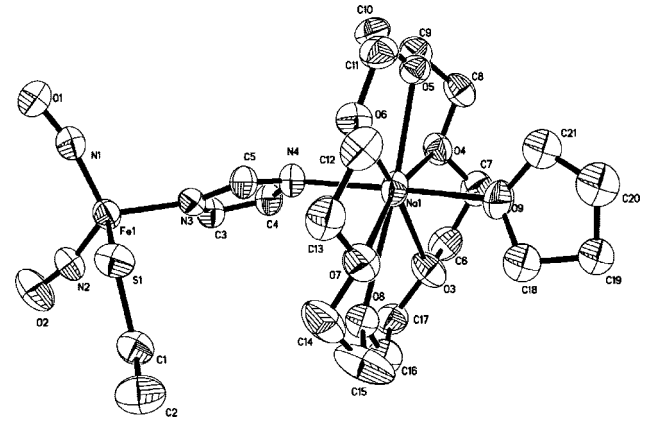

Figure 7. ORTEP drawing and labeling scheme of $[(NO)_2Fe(C_3H_3N_2)(SEt)]^-$ (**4**) unit in $[Na\text{-}18\text{-}crown\text{-}6\text{-}ether]^+$ salt with thermal ellipsoids drawn at 50% probability. Selected bond distances (Å) and angles (deg) are as follows: Fe(1)−N(1) 1.675(3); Fe(1)−N(2) 1.681(3); Fe(1)−N(3) 2.001(2); Fe(1)−S(1) 2.2469(9); O(1)−N(1) 1.178(3); O(2)−N(2) 1.171(3); N(1)−Fe(1)−N(2) 117.02(14); N(1)−Fe(1)−N(3) 111.13(11); N(2)−Fe(1)−N(3) 107.58(11); N(1)−Fe(1)−S(1) 103.09(11); N(2)−Fe(1)−S(1) 109.00(9); N(3)−Fe(1)−S(1) 108.74(7); O(1)−N(1)−Fe(1) 168.0(3); O(2)−N(2)−Fe(1) 166.7(3).

2.237(2)/2.2469(9)/2.265(2) Å for complexes **3**−**5** are presumably caused by electronic perturbation from the stronger electron-donating alkylthiolate-coordinated ligands of complexes $[(NO)_2Fe(SR)_2]^-$ (R = ^{t}Bu, Et) to the weaker electron-donating deprotonated imidazole-coordinated ligand of complexes **3**−**5** (Table 3). Specifically, the shortening of the Fe−S distance of complexes **3**–**5** was employed to reimburse the electron deficiency induced by the less electron-donating deprotonated imidazole-coordinated ligand to stabilize the anionic $\{Fe(NO)_2\}^9$ DNICs **3**–**5**. This result is consistent with the stronger electron-donating thiolates $[RS]^-$ promoting ligand exchange of complex **2** to produce the stable complexes **3**–**5**[12] and further protonation of complexes **4** and **5** to produce complexes $[(NO)_2Fe(SR)_2]^-$ (R = Et, Ph) observed in this study.

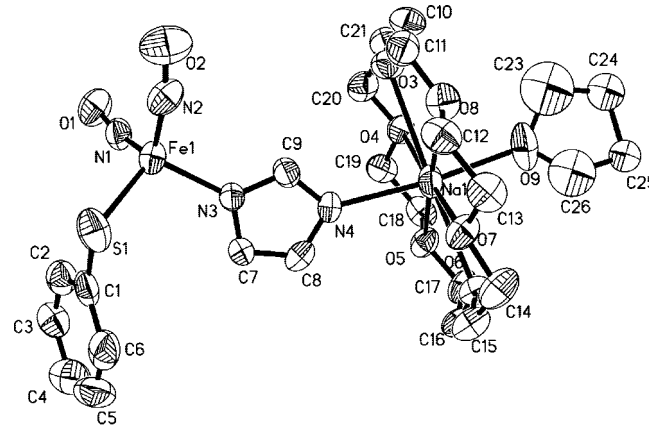

Figure 8. ORTEP drawing and labeling scheme of $[(NO)_2Fe(C_3H_3N_2)(SPh)]^-$ (**5**) unit in $[Na\text{-}18\text{-}crown\text{-}6\text{-}ether]^+$ salt with thermal ellipsoids drawn at 50% probability. Selected bond distances (Å) and angles (deg) are as follows: Fe(1)−N(1) 1.701(6); Fe(1)−N(2) 1.668(7); Fe(1)−N(3) 2.000(5); Fe(1)−S(1) 2.265(2); O(1)−N(1) 1.172(7); O(2)−N(2) 1.181(8); N(1)−Fe(1)−N(2) 110.2(3); N(1)−Fe(1)−N(3) 110.8(2); N(2)−Fe(1)−N(3) 108.6(3); N(1)−Fe(1)−S(1) 112.9(2); N(2)−Fe(1)−S(1) 107.5(2); N(3)−Fe(1)−S(1) 106.57(17); O(1)−N(1)−Fe(1) 165.1(5); O(2)−N(2)−Fe(1) 164.4(6).

Table 3. Selected Fe−S and $Fe-N_{(Im\text{-}H)}$ (Im-H = Deprotonated Imidazole) Bond Lengths (Å) for the Anionic $\{Fe(NO)_2\}^9$ DNICs[16]

complex	Fe−S (Å)	Fe−N(Im-H) (Å)
2		1.974(3), 1.978(3)
3	2.237(2)	1.984(6)
4	2.2469(9)	2.001(2)
5	2.265(2)	2.000(5)
$[(NO)_2Fe(S^tBu)_2]^-$	2.2752(11), 2.2839(8)	
$[(NO)_2Fe(SEt)_2]^-$	2.2659(19), 2.283(2)	
$[(NO)_2Fe(SPh)_2]^-$	2.2814(6), 2.3030(6)	

Conclusion and Comments

Studies on the dinitrosyliron complexes **2**–**5** containing the deprotonated imidazole-coordinated ligand(s) and the interconversion among complexes **2**−**5** and $[(NO)_2Fe(SR)_2]^-$ (R = ^{t}Bu, Et, Ph) have led to the following results, including certain results from earlier studies.[6b,c,12]

(1) Compared to the formation of $[(NO)_2Fe(SR)_2]^-$ by reaction of **4** and **5** and HSR (R = Et, Ph), the steric effects of the coordinated ligands in the coordination sphere from complex **3** to $[(NO)_2Fe(S^tBu)_2]^-$ overwhelm the electronic effects expected in the ligand-displacement reaction of DNICs, rationalizing that DNIC **3** is inert to the further addition of HS^{t}Bu.

(2) The more electron-donating functionality of thiolate(s), compared to the deprotonated imidazole, is responsible for the transformation of complex **2** into complexes **3**−**5** and complex **5** into $[(NO)_2Fe(SPh)_2]^-$ by the deprotonated imidazole−thiolate exchange reaction. It is presumed that the electronic deficiency of $\{Fe(NO)_2\}$ core induced by the less electron-donating deprotonated imidazole- and $[SPh]^-$-coordinated ligand of complexes **2** and **5**, respectively, triggers the coordination of $[SR]^-/[SPh]^-$ to the $\{Fe(NO)_2\}$ core of complexes **2** and **5**, and the subsequent elimination of the coordinated deprotonated imidazole yields complexes **3**–**5** and $[(NO)_2Fe(SPh)_2]^-$, respectively. This rationalization also explains that the stronger electron-donating thiolates $[R'S]^-$, compared to the coordinated thiolate/imidazole ligands of the dinitrosyliron complexes $[(RS)_2Fe(NO)_2]^-/[(RS)(Im)Fe(NO)_2]$ (Im= imidazole), respectively,

Scheme 3

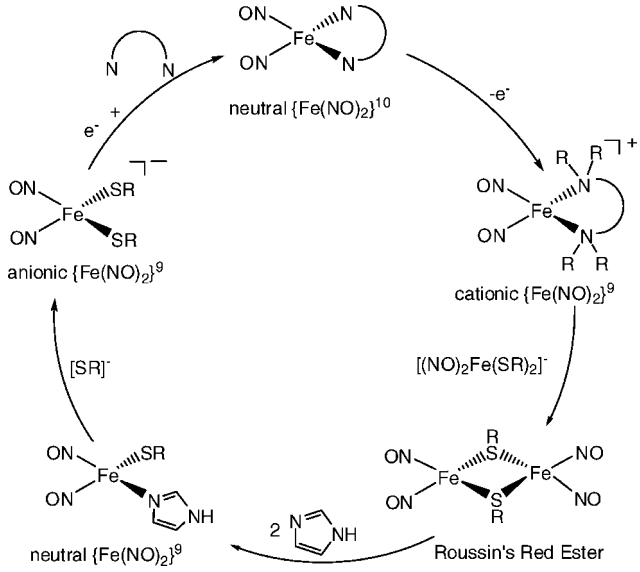

promote ligand exchange to yield the stable DNICs $[(R'S)_2Fe(NO)_2]^-$ observed in the previous study.[6b,12] Conclusively, the distinct electron-donating ability of thiolates may serve to regulate the stability of DNICs and the ligand-substitution reactions of DNICs.

(3) The EPR spectrum of DNIC **2** exhibits the well-resolved nine-line EPR signal with $g = 2.027$ and the coupling constants $a_{N(NO)} = 2.20$ and $a_{N(Im-H)} = 3.15$ G at 298 K. In comparison, the EPR spectrum of complex **4** exhibits the well-resolved 11-line signals with $g = 2.027$ and the hyperfine coupling constants $a_{N(NO)} = 2.50$, $a_{N(Im)} = 4.10$, and $a_H = 1.55$ G derived from coupling with H of the coordinated S−CH_2−Me group (Table 2). The detailed spectroscopic analysis (EPR spectrum (the pattern of hyperfine splitting) and IR ν_{NO} spectrum ($\Delta\nu_{NO}$ = separation of NO stretching frequencies; $\Delta\nu_{NO}$, ∼62 cm^{-1} for **2** vs ∼50 cm^{-1} for **3**–**5** vs ∼43 cm^{-1} for $[(NO)_2Fe(S^tBu)_2]^-$/$[(NO)_2Fe(SEt)_2]^-$/$[(NO)_2Fe(SPh)_2]^-$)) may provide a superior level of insight on discrimination of the anionic $\{Fe(NO)_2\}^9$ DNICs containing the different ligations [N,N]/[N,S]/[S,S].

(4) Compared to the interconversions among the variety of electronic states, i.e., the neutral $\{Fe(NO)_2\}^{10}$ DNICs, the cationic $\{Fe(NO)_2\}^9$ DNICs, the neutral $\{Fe(NO)_2\}^9$ DNICs, the anionic $\{Fe(NO)_2\}^9$ DNICs, and Roussin's red ester (RRE) observed in the previous study (Scheme 3),[6,12,16] the facile transformation of the anionic $\{Fe(NO)_2\}^9$ DNICs containing the various ligation modes [N,N]/[N,S]/[S,S] was demonstrated in this systematic study.

We expect that syntheses of the anionic $\{Fe(NO)_2\}^9$ DNICs **2**−**5** may support/decipher the existence of the protein-bound $\{Fe(NO)_2\}$-$[N_{His},N_{His}]$ and $\{Fe(NO)_2\}$-$[N_{His}, S_{Cys}]$ ligation DNICs in the biological system and the interconversion of the anionic $\{Fe(NO)_2\}^9$ DNICs **2**−**5** and $[(NO)_2Fe(S^tBu)_2]^-$/$[(NO)_2Fe(SEt)_2]^-$/$[(NO)_2Fe(SPh)_2]^-$ will be comparable in vitro/in vivo to that of the biological system.[4,5]

Experimental Section

Manipulation, reactions, and transfers were conducted under nitrogen according to Schlenk techniques or in a glovebox (nitrogen gas). Solvents were distilled under nitrogen from appropriate drying agents (diethyl ether from sodium benzophenone, acetonitrile from $CaH_2-P_2O_5$, methylene chloride from CaH_2, hexane and tetrahydrofuran (THF) from sodium benzophenone) and stored in dried N_2-filled flasks over 4 Å molecular sieves. Nitrogen was purged through these solvents before use. Solvent was transferred to the reaction vessel via stainless steel cannula under positive pressure of N_2. [Na-18-crown-6-ether][$(NO)_2Fe(SC_7H_4SN)_2$] (**1**) and Roussin's red ester [Fe(μ-SR)$(NO)_2]_2$ (R= ^{t}Bu, Et, Ph) were synthesized and characterized by published procedures.[12] Infrared spectra of the ν(NO) stretching frequencies were recorded on a PerkinElmer model Spectrum One B spectrometer with sealed solution cells (0.1 mm, KBr windows) or KBr solid. UV–vis spectra were recorded on a Jasco V-570 spectrometer. Analyses of carbon, hydrogen, and nitrogen were obtained with a CHN analyzer (Heraeus).

Preparation of [Na-18-crown-6-ether][$(NO)_2Fe(C_3H_3N_2)_2$] (2). Complexes [Na-18-crown-6-ether][$(NO)_2Fe(SC_7H_4SN)_2$] (**1**) (0.368 g, 0.5 mmol) and sodium imidazole ([Na][$C_3H_3N_2$]) (0.091 g, 1.0 mmol) were dissolved in THF (10 mL) and stirred overnight under nitrogen at ambient temperature. The reaction was monitored with FTIR. The IR ν_{NO} stretching frequencies shifted from 1767 and 1717 s to 1774 and 1712 s cm^{-1}. The reaction solution was filtered through Celite and dried under vacuum. The isolated dark-brown solid was redissolved in CH_2Cl_2 and the extremely moisture-sensitive, dark-brown crystals [Na-18-crown-6-ether]-[$(NO)_2Fe(C_3H_3N_2)_2$] (**2**) (yield 0.126 g, 47%), suitable for X-ray crystallography, were then isolated from nitrogen purge of CH_2Cl_2 solution of complex **2** at ambient temperature. IRν_{NO}: 1774 s, 1712 s cm^{-1} (THF); 1785 s, 1717 s cm^{-1} (CH_2Cl_2). Absorption spectrum (THF) [nm, λ_{max} (M^{-1} cm^{-1}, ϵ)]: 322 (3560), 441 (500), 710 (155). Anal. Calcd for $C_{18}H_{30}N_6NaO_8Fe$: C, 40.23; H, 5.82; N, 15.64. Found: C, 39.64; H, 5.60; N, 15.03.

Preparation of [Na-18-crown-6-ether][$(NO)_2Fe(C_3H_3N_2)$-(S^tBu)] (3). Complex **2** (0.269 g, 0.5 mmol) was dissolved in THF under nitrogen at ambient temperature. The 56.3 μL of *tert*-butylthiol (0.5 mmol) was diluted to 5 mL using THF. The diluted *tert*-butylthiol solution was injected drop by drop into the THF solution of complex **2**, and the stretching frequencies ν_{NO} shifting from 1774 and 1712 s cm^{-1} (complex **2**) to 1741 and 1690 s cm^{-1} (THF) implicated the formation of [Na-18-crown-6-ether]-[$(NO)_2Fe(C_3H_3N_2)(S^tBu)$] (**3**). The solution was concentrated under purge of N_2, and hexane was then added to precipitate the brown solid [Na-18-crown-6-ether][$(NO)_2Fe(C_3H_3N_2)(S^tBu)$] (**3**) (yield 0.238 g, 85%). Diffusion of hexane into the THF solution of complex **3** under nitrogen at ambient temperature led to the brown crystals suitable for X-ray diffraction. IRν_{NO}: 1741 s, 1690 s cm^{-1} (THF). Absorption spectrum (THF) [nm, λ_{max} (M^{-1} cm^{-1}, ϵ)]: 364 (3511), 433 (1950), 726 (226). Anal. Calcd for $C_{19}H_{36}N_4NaO_8SFe$: C, 40.79; H, 6.49; N, 10.02. Found: C, 40.67; H, 6.49; N, 10.31. Alternatively, complexes [Fe(μ-S^tBu)$(NO)_2]_2$ (0.205 g, 0.5 mmol) and [Na-18-crown-6-ether][$C_3H_3N_2$] (0.355 g, 1 mmol) were dissolved in THF (10 mL) and stirred for 10 min under nitrogen at ambient temperature. The reaction was monitored with FTIR and the IR ν_{NO} shifting from 1805 vw, 1771, and 1745 s to 1741s and 1690 s cm^{-1} were observed, consistent with the formation of complex **3**.

Preparation of [Na-18-crown-6-ether][$(NO)_2Fe(C_3H_3N_2)(SEt)$] (4). Complex **2** (0.269 g, 0.5 mmol) was dissolved in THF under nitrogen at ambient temperature. The 37 μL of ethanethiol (0.5

mmol) was diluted to 5 mL using THF. The diluted ethanethiol THF solution was injected by syringe drop by drop into the THF solution of complex **2.** The reaction was monitored with FTIR. After addition of diluted ethanethiol, IR spectrum displayed two absorption bands (ν_{NO}, 1741 s, 1693 s cm^{-1} (THF)) assigned to the formation of [Na-18-crown-6-ether][$(NO)_2Fe(C_3H_3N_2)$(SEt)] (**4**). The solution was concentrated and hexane was added to precipitate the dark-brown solid [Na-18-crown-6-ether][$(NO)_2Fe(C_3H_3N_2)$(SEt)] (**4**) (yield 0.186 g, 70%). Diffusion of hexane into the THF solution of complex **4** under nitrogen at ambient temperature led to the dark-brown crystals. IR ν_{NO}: 1741 s, 1693 s cm^{-1} (THF). Absorption spectrum (THF) [nm,λ_{max} (M^{-1} cm^{-1}, ϵ)]: 371 (2078), 437 (1428), 741 (279). Anal. Calcd for $C_{17}H_{32}N_4NaO_8SFe$: C, 38.42; H, 6.07; N, 10.55. Found: C, 39.82; H, 6.54; N, 10.95. Alternatively, complexes [Fe(μ-SEt)$(NO)_2]_2$ (0.177 g, 0.5 mmol) and [Na-18-crown-6-ether][$C_3H_3N_2$] (0.355 g, 1 mmol) were dissolved in THF (10 mL) and stirred for 10 min under nitrogen at ambient temperature. The reaction was monitored with FTIR, and the IR ν_{NO} shifting from 1809 vw, 1774, and 1749 s to 1742 and 1693 s cm^{-1} were observed, consistent with the formation of complex **4**.

Preparation of [Na-18-crown-6-ether][$(NO)_2Fe(C_3H_3N_2)$(SPh)] (5). Complex **2** (0.269 g, 0.5 mmol) was dissolved in THF under nitrogen at ambient temperature. The 51.3 μL of thiophenol (0.5 mmol) was diluted to 2 mL using THF. The diluted thiophenol THF solution was injected by syringe drop by drop into the THF solution of complex **2** at room temperature. After the diluted thiophenol THF solution was completely added, two absorption bands (ν_{NO}, 1708 s, 1760 s cm^{-1} (THF)), assigned to the formation of [Na-18-crown-6-ether][$(NO)_2Fe(C_3H_3N_2)$(SPh)] (**5**), appeared. The solution was concentrated and hexane was added to precipitate the red-brown solid [Na-18-crown-6-ether][$(NO)_2Fe(C_3H_3N_2)$(SPh)] (**5**) (yield 0.232 g, 80%). Diffusion of hexane into the THF solution of complex **5** under nitrogen at ambient temperature led to the red-brown crystals, suitable for single-crystal X-ray diffraction. IR ν_{NO}: 1760 s, 1708 s cm^{-1} (THF). Absorption spectrum (THF) [nm, λ_{max} (M^{-1} cm^{-1}, ϵ)]: 457 (2531), 521 (2054), 754 (1141). Anal. Calcd for $C_{21}H_{32}N_4NaO_8SFe$: C, 43.53; H, 5.57; N, 9.67. Found: C, 43.18; H, 5.63; N, 9.67. Alternatively, complexes [Na-18-crown-6-ether][$C_3H_3N_2$] (0.355 g, 1 mmol) and [Fe(μ-SPh)$(NO)_2]_2$ (0.225 g, 0.5 mmol) were dissolved in THF (10 mL) and stirred for 10 min under nitrogen at ambient temperature. The reaction was monitored with FTIR, and the IR ν_{NO} shifting from 1814 vw, 1783, and 1757 s to 1760 and 1708 s cm^{-1} were observed, consistent with the formation of complex **5**.

Reaction of Complex 4 and Ethanethiol (or Reaction of Complex 5 and Thiophenol). Complex **4** (0.270 g, 0.5 mmol) (or complex **5** (0.289 g, 0.5 mmol)) was dissolved in THF under nitrogen at ambient temperature. The 37 μL of ethanethiol (0.5 mmol) (or thiophenol (51.3 μL, 0.5 mmol)) was diluted to 5 mL using THF. The diluted ethanethiol (or thiophenol) THF solution was injected slowly into the THF solution of complex **4** (or complex **5**) at room temperature. The mixture was stirred at ambient temperature and monitored with FTIR. IR spectrum (ν_{NO}, 1714 s, 1674 s cm^{-1} (THF)) indicated the formation of the known [Na-18-crown-6-ether][$(NO)_2Fe(SEt)_2$] (or [Na-18-crown-6-ether]-[$(NO)_2Fe(SPh)_2$] (ν_{NO}, 1739 s, 1695 s cm^{-1} (THF))).[16a]

Reaction of Complex 5 and [Na][SPh]. Complex **5** (0.289 g, 0.5 mmol) and [Na][SPh] (0.066 g, 0.5 mmol) were dissolved in THF (7 mL) and stirred for 10 min under nitrogen at ambient temperature. The reaction was monitored with FTIR and the IR ν_{NO} stretching frequencies shifting from 1760 and 1708 s cm^{-1} to 1739 and 1695 s cm^{-1} were observed, consistent with the formation of the well-known [Na-18-crown-6-ether][$(NO)_2Fe(SPh)_2$].[16a,c]

EPR Measurements. EPR measurements were performed at X-band using a Bruker EMX spectrometer equipped with a Bruker TE102 cavity. The microwave frequency was measured with a Hewlett-Packard 5246L electronic counter. At 298 K, X-band EPR spectra of complexes **2**, **3**, and **4** in THF were obtained with a microwave power of 19.971, 12.570, and 15.863 mW, frequency at 9.605, 9.601, and 9.603 GHz, and modulation amplitude of 0.80 G at 100.00 kHz, respectively. At 77 K, the EPR spectra of complexes **2**, **3**, and **4** frozen in THF were obtained with a microwave power of 19.922, 19.873, and 19.873 mW, frequency at 9.604, 9.601, and 9.605 GHz, and modulation amplitude of 0.8 G at 100 KHz, respectively.

Magnetic Measurements. The magnetic data were recorded on a SQUID magnetometer (MPMS5 Quantum Design Company) under 0.5 T external magnetic field in the temperature range 2–300 K. The magnetic susceptibility data were corrected with temperature independent paramagnetism (TIP, 2×10^{-4} cm^3 mol^{-1}), and ligands' diamagnetism by the tabulated Pascal's constants.

Crystallography. Crystallographic data and structure refinements parameters of complexes **2**–**5** are summarized in the Supporting Information. The crystals chosen for X-ray diffraction studies measured $0.4 \times 0.24 \times 0.09$ mm^3 for complex **2**, $0.32 \times 0.19 \times 0.1$ mm^3 for complex **3**, $0.42 \times 0.20 \times 0.05$ mm^3 for complex **4**, and $0.22 \times 0.14 \times 0.08$ mm^3 for complex **5**. Each crystal was mounted on a glass fiber and quickly coated in epoxy resin. Unit-cell parameters were obtained by least-squares refinement. Diffraction measurements were carried out on a SMART CCD diffractometer with graphite-monochromated Mo Kα radiation (λ = 0.7107 Å). Least-squares refinement of the positional and anisotropic thermal parameters of all non-hydrogen atoms was based on F^2. A SADABS absorption correction was made.[18] The SHELXTL structure refinement program was employed.[19] In the case of complexes **3**–**5**, the coordinated solvent THF was found to be disordered, and positions were modeled with positional coordinates refined.

Acknowledgment. We gratefully acknowledge financial support from the National Science Council of Taiwan.

Supporting Information Available: Figure showing the X-ray structure of **2** and tables listing crystallographic information of complexes **2**−**5**; X-ray crystallographic files in CIF format for the structure determinations of [Na-18-crown-6-ether]-[$(NO)_2Fe(C_3H_3N_2)_2$], [THF-Na-18-crown-6-ether][$(NO)_2Fe(C_3H_3N_2)$(S^{t}Bu)], [THF-Na-18-crown-6-ether][$(NO)_2Fe(C_3H_3N_2)$(SEt)], and [THF-Na-18-crown-6-ether][$(NO)_2Fe(C_3H_3N_2)$(SPh)]. This material is available free of charge via the Internet at http://pubs.acs.org.

IC702000Y

(18) Sheldrick, G. M. *SADABS, Siemens Area Detector Absorption Correaction Program*; University of Göttingen: Göttingen, Germany, 1996.
(19) Sheldrick, G. M. *SHELXTL, Program for Crystal Structure Determination*; Siemens Analytical X-ray Instruments Inc.: Madison, WI, 1994.